Journal of Electronic Materials, Vol. 24, No. 10, 1995

Regular Issue Paper

Electron-Concentration Dependence of Absorption and Refraction in n-$In_{0.53}Ga_{0.47}As$ Near the Band-Edge

D. HAHN, O. JASCHINSKI, H.-H. WEHMANN, and A. SCHLACHETZKI

Institut für Halbleitertechnik, Technische Universität Braunschweig, Hans-Sommer-strasse 66, D-38106 Braunschweig, Germany

M. VON ORTENBERG

Institut für Physik, Lehrstuhl Magnetotransport, Humboldt Universität Berlin, Invalidenstrasse 110, D-10115 Berlin, Germany

The optical constants of InGaAs were determined as a function of electron concentration in the range from 10^{15} to 2×10^{19} cm^{-3} by reflectance- and transmission-spectroscopy. A pronounced shift of the fundamental absorption edge toward shorter wavelengths with increasing doping concentration was found. The experimental results can be satisfactorily explained by band-filling and band-gap shrinkage.

Key words: Absorption coefficient, band-gap shift, electron-concentration dependence, n-$In_{0.53}Ga_{0.47}As$, refractive index

INTRODUCTION

Due to its superior electronic properties the ternary semiconductor $In_{0.53}Ga_{0.47}As$ (InGaAs for short), lattice matched to InP, has found wide application in high-speed electronic and optoelectronic devices. In order to model such optoelectronic devices and to understand their performance, a precise knowledge of the optical properties of InGaAs near its band-edge is necessary. In general, the refractive index $\bar{n}$ and the absorption coefficient $\bar{\alpha}$ are functions of the carrier-concentration. In several n-type semiconductors, the fundamental absorption edge shifts to shorter wavelengths with increasing electron concentration. This phenomenon, the so-called Burstein-Moss effect,[1] has been explained by band-filling. Since it depends on the curvature and density of states of the conduction-band, it is more pronounced in semiconductors with small effective mass. Therefore, it can be expected that among the whole range of $In_{1-x}Ga_xAs_yP_{1-y}$ alloys, lattice matched to InP, InGaAs will show the strongest variation of the optical properties near the band-gap. However, compared to experimental results, the calculations of the band-gap variation based solely on the Burstein-Moss effect, i.e. the penetration of the Fermi-level into the conduction band, always lead to considerably larger energy shifts. This deviation was attributed to the shrinkage of the fundamental band-gap due to electron-impurity and electron-electron interactions. Thus, for theoretical description of the variation of the optical properties of InGaAs with doping concentration band-filling as well as band-gap shrinkage have to be taken into consideration.

In the past, the optical constants of InGaAs were determined by several authors using undoped material.[2-6] Humphreys et al.[7] measured the absorption coefficient for two InGaAs layers with different hole concentrations. Besides these investigations, no experimental data are available for the carrier-concen-

(Received February 23, 1995; revised May 15, 1995)

Table I. Thickness d, Electron Concentration n, and Room-Temperature Mobility μ of the Investigated InGaAs Samples

Sample #	d (μm)	n (cm^{-3})	μ(cm^2/Vs)
1	3.8	2.8×10^{15}	9140
2	3.3	7.8×10^{15}	9540
3	2.1	1.1×10^{16}	9380
4	2.6	5.3×10^{16}	7740
5	3.9	1.1×10^{17}	7700
6	2.5	5.4×10^{17}	5520
7	4.2	1.9×10^{18}	4200
8	3.9	6.9×10^{18}	3300
9	3.8	1.3×10^{19}	2600
10	2.5	1.8×10^{19}	2160

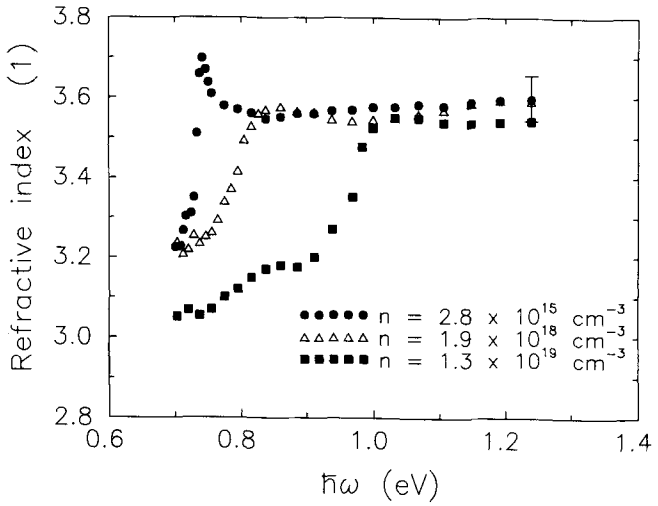

Fig. 1. Refractive index spectra of n-$In_{0.53}Ga_{0.47}As$ of different electron concentrations.

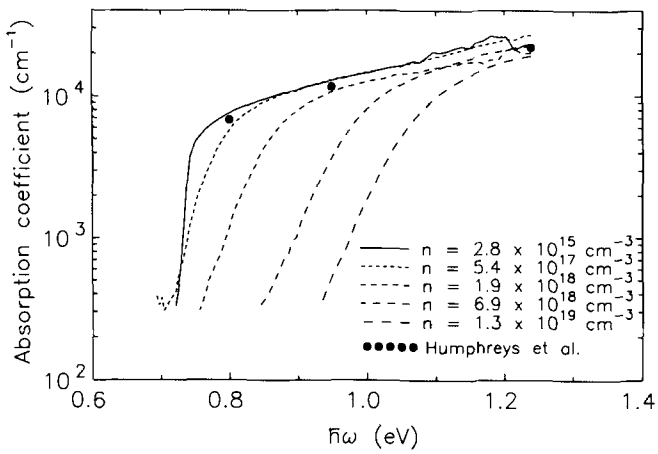

Fig. 2. Absorption spectra of n-$In_{0.53}Ga_{0.47}As$ of different electron concentrations.

tration dependence of absorption coefficient and refractive index of InGaAs. It is our aim to fill this gap.

EXPERIMENT

The samples investigated in this work were grown by liquid-phase epitaxy (LPE) on (100) InP:Fe using a standard graphite sliding boat.[8] We employed as dopant tin for the medium doping range, and above 2×10^{18} cm^{-3} tellurium was used. The thickness of the lattice matched InGaAs layers was obtained microscopically with stained cleavage planes. By van der Pauw measurements, the electron concentration and mobility were determined. Table I lists the electrical characteristics and the thickness of the samples. To evaluate the absorption coefficient and the index of refraction, the spectral transmittance and reflectance of the samples were measured at normal and near normal incidence, respectively. The angle of incidence of the latter case was less than eight degrees. The optical setup consists of a monochromator with a 600 l/mm grating for the spectral range of 0.6–2 μm and a 300 W current-stabilized xenon lamp as a light source. A calibrated germanium photodiode with a diameter of 10 mm was used as a detector. To obtain the reflectance of the samples, the measured spectra were compared to a known reflectance spectrum of a freshly deposited gold mirror. Before the investigations, the rough back surface of the samples was polished on a Pellon disk using an 0.4% bromine-methanol solution. With this preparation, errors due to the scattering of light were minimized to below 5% as secured in the transparent regime of the samples.

The absorption coefficient $\bar{\alpha}$ and the refractive index $\bar{n}$ were calculated from the transmission and reflection spectra using a matrix formalism for the parallel-plate system taking into account multiple reflections.[9] Interference effects were neglected because of inevitable thickness inhomogeneities of the LPE grown layers. According to Table I, the thickness of the examined InGaAs layers range from 2 to 4 μm. With our optical setup, this corresponds to an easily accessible range for the absorption coefficient between 3×10^2 and 2×10^4 cm^{-1}.

RESULTS AND DISCUSSION

Figure 1 presents the measured refractive index of InGaAs for three different electron concentrations. Since the reflectivity measurements are very sensitive to the roughness of the InGaAs surface, the relative error is about $\Delta \bar{n} = \pm 0.04$ as indicated by the vertical error bar. The spectral course of the refractive index is in agreement with that calculated from the absorption, presented later, by applying the Kramers-Kronig relation.[10] For low electron concentrations ($n = 2.8 \times 10^{15}$ cm^{-3}), the refractive index shows a pronounced resonance at the energy where the absorption coefficient changes most rapidly. This peak flattens out more and more for increasing electron concentrations. Due to the shift of the band-gap, the decrease of the refractive index occurs at higher energies. The refractive indices at the band-edge determined by Chandra et al.[3] ($\bar{n} = 3.58$) and Burkhard et al.[2] ($\bar{n} = 3.55$) for undoped InGaAs support our measurements.

The absorption coefficient of n-InGaAs is displayed for different electron concentrations n in Fig. 2. The agreement with the results of Humphreys et al.[7] for undoped InGaAs at the photon energies $\hbar\omega$ of 0.8, 0.95, and 1.24 eV (corresponding to wavelengths of

1.55, 1.3, and 1.0 μm, solid symbols) is good. As expected, a distinct shift of the fundamental absorption edge toward higher energies (Burstein shift due to band-filling) occurs with increasing carrier concentration. For example, the absorption coefficient of InGaAs at a wavelength of 1.3 μm is less than 300 cm^{-1} for an electron concentration of 1.8×10^{19} cm^{-3} (not shown in Fig. 2). In comparison with n-InP[11] and n-InGaAsP,[12] the shift of the fundamental absorption edge is more significant which results from the smaller effective density of states in the conduction band of InGaAs. The data in Fig. 2 show an exponential absorption tail, which can be described by the Urbach rule[13]

$$\bar{\alpha} = \bar{\alpha_u} \exp\left(-\frac{E_g - \hbar\omega}{E_u}\right) \quad (1)$$

E_u (Urbach energy)[14] and $\bar{\alpha_u}$ are fitting parameters and E_g is the band-gap of InGaAs. This absorption tail is assumed to result from internal electrical fields caused by phonons, impurities, and excitons.[15] The Urbach energy is temperature dependent, which is often approximated as[16]

$$E_u = \frac{\hbar\omega_p}{2\sigma_0}\left(\tanh\left[\frac{\hbar\omega_p}{2kT}\right]\right)^{-1} \quad (2)$$

σ_0 is a constant which can be related to the temperature dependence of the band-gap.[17] $\hbar\omega_p$ corresponds in some cases to the energy of the phonons involved in the formation of the absorption tail.[16]

It is found from Fig. 2 that the slope of the absorption tail corresponding to the Urbach energy

$$E_u = \left[d(\ln\bar{\alpha})/d(\hbar\omega)\right]^{-1} \quad (3)$$

increases with increasing doping concentration as also found with GaAs.[14] Figure 3 gives this dependence for InGaAs at room temperature. In this figure, the Urbach energy is presented in dependence on the cubic root of the reciprocal electron concentration which is a measure of the average distance between donors. The measured values (solid squares) are compared to the results by Rajalakshmi and Arora[18] for n-InGaAsP (open triangles), calculated for 300K by use of (2) with $\hbar\omega_p$ = 41.5 meV.[18] In order to determine E_u for 300K based on the measurements by Rajalakshmi and Arora[18] taken at 80K we included the temperature dependence of σ_0 by $\sigma_0 = 3k/(-dE_g/dT)$.[17] Given $E_g(T)$,[18] we find σ_0 (80K) = 1.45 and σ_0 (300K) = 0.96.

Up to electron concentrations of about 10^{17} cm^{-3}, the Urbach energy in InGaAs is approximately 13 meV (see Fig. 3), which is slightly smaller than the value for InGaAsP (16 meV). Beyond 10^{17} cm^{-3}, the Urbach energy increases with $n^{1/3}$ for both compositions. One reason for the doping dependence of the Urbach energy is the increasing perturbation of the band edge by the internal electrical field fluctuations of the impurities,[15] leading to tails in the density of states. Since the Urbach energy decreases proportional to the cubic root of the reciprocal electron concentration, it can be expected that this interaction depends on the mean distance of the impurities. Alternatively, Economou et al.[19] showed that the Urbach energy is related to potential fluctuations on a microscopic scale. Following this model the doping dependence of the Urbach energy is the result of impurity disorder.

In order to determine the effective energy $E_{g,opt}$ for optical band-to-band transitions as a function of the electron concentration, we used the functional dependence of the absorption coefficient $\bar{\alpha}$ on the photon energy $\hbar\omega$. Assuming a direct band gap, a nondegenerate semiconductor and parabolic bands this dependence can be written as[4]

$$\bar{\alpha} \propto \frac{\left(\hbar\omega - E_{g,opt}\right)^{1/2}}{\hbar\omega}. \quad (4)$$

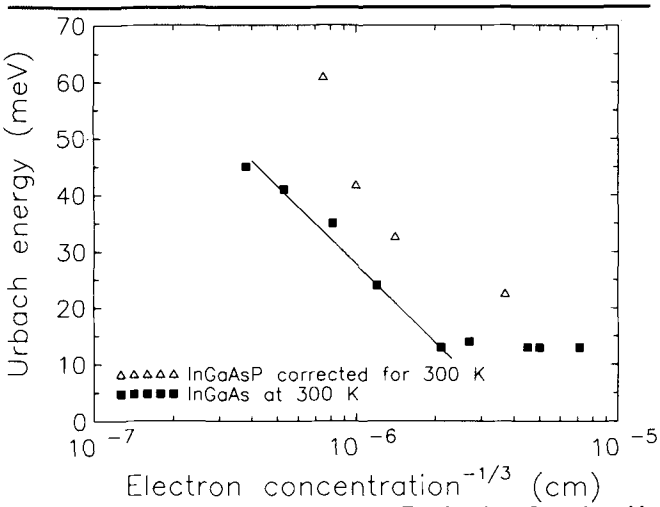

Fig. 3. Variation of the Urbach energy E_u of n-$In_{0.53}Ga_{0.47}As$ with electron concentration. The values for InGaAs are compared with the results by Rajalakshmi and Arora for $In_{0.72}Ga_{0.28}As_{0.6}P_{0.4}$.

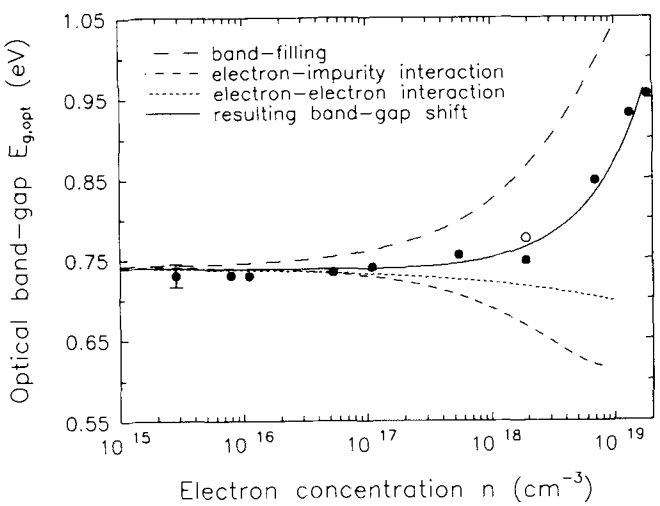

Fig. 4. Variation of the energy for optical band-to-band transitions in InGaAs as a function of electron concentration. The contributions of the band-filling and the band-gap shrinkage (electron-impurity and electron-electron interaction) to the resulting band-gap shift are presented as dashed curves. The experimental results are obtained from absorption (solid symbols) and photoluminescence (open symbols) measurements.

In the case of a degenerate direct band-gap semiconductor, the absorption coefficient can be described by[11]

$$\overline{\alpha} \propto \frac{\left(\hbar\omega - E_{g,opt}\right)^2}{\hbar\omega} \tag{5}$$

By plotting $(\overline{\alpha}\hbar\omega)^2$ or $(\overline{\alpha}\hbar\omega)^{1/2}$ vs photon energy and by extrapolating the linear part of the absorption curve $E_{g,opt}$ was obtained. In Fig. 4, the results are represented as solid symbols. For a theoretical explanation, we considered the penetration of the Fermi level into the conduction band (band filling) and the band-gap shrinkage due to electron-impurity interaction (band tailing) and electron-electron interaction (Coulomb interaction). The energy for direct band-to-band transitions $E_{g,opt}$ was taken as

$$E_{g,opt} = E_{g0} + E_F - E_{bt} - E_{int} \tag{6}$$

with E_{g0} being the energy gap of undoped InGaAs, E_F the Fermi energy relative to the bottom of the conduction band, E_{bt} and E_{int} the energies for the band-gap shrinkage due to band tailing and due to Coulomb interaction, respectively.

In order to calculate E_F, we used the expression given by Raymond et al.[20]

$$E_F = (3\pi^2)^{2/3}\left(\frac{\hbar^2}{2m_0^*}\right)\left(1-\frac{\Phi}{E_g}\right)n^{2/3}$$

$$\Phi = \alpha\chi(3\pi^2)^{2/3}\left(\frac{\hbar^2}{2m_0^*}\right)n^{2/3}. \tag{7}$$

m_0^* denotes the effective mass at the bottom of the conduction band. The nonparabolicity factor α can be calculated after Kane's three-band model.[11] This approach is supported by experiments for large values of n.[20,21] In the calculation of α for the analysis of our experiments we used $E_{g0} = 0.741$ eV for the band-gap energy,[22] $\Delta = 0.312$ eV for the split-off valence-band energy[23] and $m_0^* = 0.041\, m_e$ (m_e free-electron mass).[24] Since E_F after this procedure vanishes for electron concentrations above 10^{19} cm^{-3}, we added an empirical correction factor χ as a fitting parameter, as proposed by Beaumont et al. for InGaAsP.[12] For a screened Coulomb potential the band-gap shrinkage due to the electron-impurity interaction can be written as[11]

$$E_{bt} = \left(\frac{\pi^{4/3}\hbar^2}{3^{1/3}}\right)n^{2/3}\left(\frac{1}{m_0^*}\right)\left(1-2\frac{\Phi}{E_{g0}}\right). \tag{8}$$

The term $(1/m_0^*)(1-2\Phi/E_{g0})$ is the conductivity effective mass where Φ takes into account the nonparabolicity of the conduction band for large n. The conductivity effective mass is synonymous with the optical effective mass.[25] Equation (8) is valid under the assumptions of a linear screening approximation and a degenerate semiconductor with nonparabolic band. For the same reasons as discussed above, the nonparabolicity contribution to E_{bt} is empirically corrected by the factor χ.

The shrinkage of the band-gap resulting from the Coulomb interaction between carriers is given by[26]

$$E_{int} = \left(\frac{e}{2\pi\epsilon_0\epsilon_r}\right)\left(\frac{3}{\pi}\right)^{1/3} n^{1/3}. \tag{9}$$

In our calculation, we used $\epsilon_r = 13.9$ for the dielectric constant.[27] In Fig. 4, the contributions to the band-gap variation in InGaAs resulting from band filling and band-gap shrinkage are presented in dependence on the electron concentration (dashed curves). The solid curve shows $E_{g,opt}$ calculated after Eq. (6) in combination with Eqs.(7)–(9) and 0.7 as the value for the fitting parameter χ. Clearly visible is the increase of the band-gap for optical band-to-band transitions for electron concentrations above 10^{18} cm^{-3}. At $n = 2\times10^{19}$ cm^{-3}, the band-gap shift is about 250 meV, which is mainly caused by band filling. The experimental results as derived from the absorption coefficients (solid dots) are in good agreement with the theory in the low and high concentration range. For $n = 2\times10^{18}$ cm^{-3}, the experimentally determined energy deviates from the calculated band-gap because in this concentration range between nondegeneracy and degeneracy of the InGaAs, none of the approximations of Eqs. (4) and (5) are valid. Therefore, we compared the bandgap derived from Eq. (4) and Eq. (5) with the results from photoluminescence measurements at room temperature. We found that the band-gap obtained from photoluminescence measurements agrees with the results from the absorption curves (not shown) with the exception of $E_{g,opt}$ at $n = 2\times10^{18}$ cm^{-3} (open symbol). This demonstrates that the experimental results can be described satisfactorily by our formalism. However, it must be stressed that we use Eq. (9) beyond the range of its validity and that we adjust Eq. (7) and Eq. (8) to our experiments by introducing the fitting parameter χ.

SUMMARY

The absorption and refraction of n-InGaAs near the band-edge were measured by reflection and transmission spectroscopy in dependence on the electron concentration. From the absorption spectra, the Urbach energy and the band-gap for optical band-to-band transitions were determined. Due to the small effective electron mass in InGaAs a strong band filling occurs leading to a shift of the fundamental band-gap with increasing electron concentration that becomes very pronounced above 10^{17} cm^{-3}. The variation of the optical band-gap with doping concentration was explained by band filling and band-gap shrinkage, which were both calculated for nonparabolic bands. For a good agreement between theory and experiment, it was necessary to correct empirically the effective electron mass following from the usual approach by Raymond et al.[20] Without this correction, the effective electron mass becomes infinite at electron concentrations greater than 10^{19} cm^{-3}.

ACKNOWLEDGMENTS

The authors wish to thank D. Rümmler for technical assistance and Dr. L. Malacky for stimulating discussions. This work was financially supported by the DBP Telekom and Volkswagen-Stiftung.

REFERENCES

1. E. Burstein, *Phys. Rev.* 93, 632 (1954).
2. H. Burkhard, H.W. Dinges and E. Kuphal, *J. Appl. Phys.* 53, 655 (1982).
3. P. Chandra. L.A. Coldren and K. E. Strege, *Electron. Lett.* 17, 6 (1981).
4. W. Kowalsky, H.-H. Wehmann, F. Fiedler and A. Schlachetzki, *Phys. Stat. Sol.* (a) 77, K75 (1983).
5. T.W. Nee and A.K. Green, *J. Appl. Phys.* 68, 5314 (1990).
6. M. Amiotti and G. Landgren, *J. Appl. Phys.* 73, 2965 (1993).
7. D.A. Humphreys, R.J. King, D. Jenkins and A.J. Moseley, *Electron. Lett.* 21, 1187 (1985).
8. F. Fiedler, H.-H. Wehmann and A. Schlachetzki, *J. Cryst. Growth* 74, 27 (1986).
9. B. Harbecke, *Appl. Phys.* B 39, 165 (1986).
10. F. Stern, *Phys. Rev. A* 133, 1653 (1964).
11. M. Bugajski and W. Lewandowski, *J. Appl. Phys.* 57, 521 (1985).
12. B. Beaumont, G. Nataf, J.C. Guillaume and C. Vèrié, *J. Appl. Phys.* 54, 5363 (1983).
13. F. Urbach, *Phys. Rev.* 92, 1324 (1953).
14. J.I. Pankove, *Phys. Rev. A* 140, 2059 (1965).
15. J.D. Dow and D. Redfield, *Phys. Rev. B* 5, 594 (1972).
16. M.V. Kurik, *Phys. Stat. Sol. (a)* 8, 9 (1971).
17. T. Skettrup, *Phys. Rev. B* 18, 2622 (1978).
18. R. Rajalakshmi and B.M. Arora, *J. Appl. Phys.* 67, 3533 (1990).
19. E.N. Economou, N. Bacalis and M.H. Cohen, *J. Non-Cryst. Solids* 97/98, 101 (1987).
20. A. Raymond, J.L. Robert and C. Bernard, *J. Phys. C* 12, 2289 (1979).
21. D. Schneider, D. Rürup, A. Plichta, H.-U. Grubert, A. Schlachetzki and K. Hansen, *Z. Phys. B* 95, 281 (1994).
22. A. Katz, ed., *Indium Phosphide and Related Materials* (Norwood: Artech House, 1992).
23. E.H. Perea, E.E. Mendez and C.G. Fonstad, *Appl. Phys. Lett.* 36, 978 (1980).
24. T.P. Pearsall, ed., *GaInAsP Alloy Semiconductors* (New York: J. Wiley and Sons, 1982).
25. V.L. Bonč-Bruevič and S.G. Kalašnikov, *Halbleiterphysik* (Berlin, Germany: VEB Deutscher Verlag der Wissenschaften, 1982).
26. J. Camassel, D. Auvergne and H. Mathieu, *J. Appl. Phys.* 46, 2683 (1975).
27. B.R. Bennett, R.A. Soref and J.A. Del Alamo, *IEEE J. of Quantum El.* 26, 113 (1990).